Theoretical and experimental study on $Mg(BH_4)_2$-$Zn(BH_4)_2$ mixed borohydrides

E.Albanese[1], G.N.Kalantzopoulos[2], J.G.Vitillo[1], E.Pinatel[1], B.Civalleri[1], S.Deledda[2], S.Bordiga[1], B.C.Hauback[2] and M.Baricco[1,*]

[1]Dipartimento di Chimica and NIS, Università di Torino, Via P.Giuria 7-9, I-10125, Torino, Italy
[2]Institute for Energy Technology, Department of Physics, P.O. Box 40, NO-2027, Kjeller, Norway

Abstract

After a screening of possible systems prone to give an enthalpy of decomposition close to 30 $kJ \cdot mol^{-1}_{H2}$, i.e. suitable for a dehydrogenation process close to room temperature and pressure, the Zn dissolution into $Mg(BH_4)_2$ has been investigated. The total energy of pure compounds and solid solutions has been computed by DFT calculations using the CRYSTAL09 code. To generate the $Mg_{(1-x)}Zn_x(BH_4)_2$ solid solution, α-phase of $Mg(BH_4)_2$ (space group $P6_122$) has been considered, with a replacement of Mg^{2+} with Zn^{2+} ions, without lowering the symmetry of the crystalline structure. On the basis of DFT results, the enthalpy of decomposition has been estimated, considering MgH_2, Zn, α-B and H_2 as products, and a value of 30 $kJ \cdot mol^{-1}_{H2}$ has been calculated for x=0.2. In order to verify the results of calculations, mixtures of $Mg(BH_4)_2$ and $ZnCl_2$ with 1.0:0.7 ratio have been ball milled, both at room temperature and in cryo-conditions. Samples have been analyzed with a combination of experimental techniques (XRD, DSC, IR-ATR, TGA, TPD, PCI). The phase mixture obtained after the synthesis strongly depends on the milling conditions. For prolonged times, the formation of Zn and $MgCl_2$ has been observed, suggesting the delivering of B-containing species during the milling. After heating, a hydrogen release, coupled with diborane delivering, has been observed for temperatures close to 100 °C, suggesting a significant decrease of the decomposition temperature with respect to pure $Mg(BH_4)_2$. Theoretical and experimental results have been discussed on the basis of the possibile reaction paths, as estimated from available thermodynamic databases.

Keywords: hydrogen storage, borohydrides, mixed cation, ab-initio.

* corresponding author: Marcello Baricco, marcello.baricco@unito.it, fax: + 39 011 670 7855

Introduction.

In comparison to other metal borohydrides, $Mg(BH_4)_2$ holds low decomposition temperature and high hydrogen gravimetric capacity (close to 15 %). However, it decomposes at 300 °C, a temperature that is still high for coupling with a proton-exchange membrane fuel cell (PEM-FC). Different approaches have been used to de-stabilize pure complex hydrides: anion substitution, cation substitution with mixed metal borohydrides formation, nanoconfinement and reactive hydride composites [1-3]. Since the first report [4], anion substitution has been suggested as a promising method to favor the thermodynamics of hydrogen sorption in complex hydrides [5-14]. For cation substitution in $Mg(BH_4)_2$, it is necessary to add a less stable pure borohydride, averaging the H-B bond strength, which depends on the M-H bond strength. For instance, a Mn-to-Mg substitution in α-$Mg(BH_4)_2$ up to 10 mol% at room temperature was recently reported [15]. Cation substitution has been confirmed by an evident decrease of the decomposition temperature of the synthesized compounds [15,16]. In $LiBH_4$, both the cationic and ionic part have been substituted simultaneously, resulting in systems with particularly reduced decomposition temperature and enhanced kinetics [17].

A first screening on the possible candidates for the cation substitution in Mg-borohydride was done performing an empirical analysis of the theoretical results obtained in ref. [18] on the mixed borohydrides with alkali metals. Because the enthalpy of decomposition of a dual-metal borohydride can be estimated by simply averaging the enthalpy of decomposition of the corresponding pure borohydrides, it appeared that Zn could be a possible candidate to be mixed with Mg. Notably, Zn^{2+} has the same charge and similar ionic radius of Mg^{2+}. It is worth noting that, even if there is no experimental evidence for the synthesis of pure $Zn(BH_4)_2$, the formation of mixed-cation based on alkali metal and zinc borohydrides has been recently reported. $LiZn_2(BH_4)_5$, $NaZn_2(BH_4)_5$ and $NaZn(BH_4)_3$ compounds, based on an interpenetrated network structure containing a $[Zn_2(BH_4)_5]^-$ ion, have been obtained [19]. On the other hand, the thermal decomposition reported for the pure compound in ref. [20], was actually obtained in presence of a significant contamination of NaCl, likely leading to the formation of mixed cation borohydrides. In all cases, an irreversible thermal decomposition, leading to Zn with delivering of B_2H_6 has been observed.

Aiming to select a possible system prone to give an enthalpy of decomposition close to 30 $kJ \cdot mol^{-1}_{H2}$, i.e. suitable for a dehydrogenation process close to room temperature and pressure, the Zn dissolution into $Mg(BH_4)_2$ has been investigated in this work. DFT calculations suggested the possible formation of solid solution. In absence of pure $Zn(BH_4)_2$, $Mg(BH_4)_2$ has been mixed with

$ZnCl_2$ by ball milling in various conditions and the resulting mixtures have been investigated by a combination of experimental techniques.

Theoretical and experimental methods

A theoretical investigation was carried out with density functional theory (DFT) calculations employing the PBE [21] exchange-correlation functional and the PBE-D* method, i.e. PBE augmented with the Grimme's DFT-D2 [22,23] empirical dispersion correction as modified for solids [24]. This contribution is based on an atom-atom pairwise –C6,ij/Rij6 (London-type correction) as implemented in the ab-inito periodic program CRYSTAL09 [25]. Crystalline orbitals are represented as linear combinations of Bloch functions (BF) and are evaluated over a regular three-dimensions mesh of points in reciprocal space. Each BF is built from local atomic orbitals (AO), which are contractions (linear combinations with constant coefficients) of Gaussian-type-functions (GTF) which, in turn, are the product of a Gaussian times a real solid spherical harmonic function. An all electron basis set has been used for all the atoms. Crystalline structures were fully optimized and then harmonic vibrational frequencies were computed. The latter, referred to Γ point, were used to estimate relevant thermodynamic quantities such as zero-point energy correction, thermal correction to enthalpy and entropy. For the mixed systems, considered the high computational cost, harmonic vibrational frequencies were not calculated. The zero-point energy correction and thermal correction to enthalpy were then obtained by interpolating those of the pure components.

Thermodynamic modeling according to the CALPHAD method has been carried out using the Thermo-Calc software. Even if pure $Zn(BH_4)_2$ has not been isolated experimentally, the Gibbs free energy of the compund (with $P6_122$ structure) was assessed on the basis of ab-initio calculations. The thermodynamic function for $Mg(BH_4)_2$ was taken from ref. [26] and the Substance database [27] was used for all the other phases.

Mixtures of α-$Mg(BH_4)_2$ and $ZnCl_2$ (99% purity, Sigma Aldrich) with 1.0:0.7 ratio were ball-milled either at room temperature or at liquid nitrogen temperature (cryomilling). Room-temperature ball milling was carried out in a Fritsch Pulverisette 6 Monomill at 400 rpm under 1 bar Ar initial pressure and using stainless steel balls and vials (ball-to-powder ratio 100:1). Pressure and temperature were monitored during milling and recorded with a Fritsch GTM/II system. Cryomilling was performed in a SPEX 6770 Freezer/Mill using a specially designed stainless steel vial, in order to minimize oxygen and nitrogen contaminations. The mass ratio between the stainless steel cylindrical impactor and the powder mixture was 15:1 and the impact frequency during milling was set at 30 Hz. All sample handling and preparation were carried out under inert Ar atmosphere

in an MBraun Unilab glove box fitted with a recirculation system and gas/humidity sensors. Oxygen and water levels were kept below 1 ppm at all times.

Powder X-Ray Diffraction (XRD) measurements have been performed in the 2θ range 2° – 90° using a laboratory diffractometer (Panalytical X'Pert Pro Multipurpose Diffractometer), equipped with Ni filtered Cu source in Debye-Scherrer geometry. Samples were sealed into boron silica glass capillaries of internal diameter 0.8 mm in nitrogen atmosphere, which give a broad peak in the pattern centered around 2θ=22°. Patterns were taken spinning capillaries at a scanning step of 0.016° and with a scan speed of 0.010°/s. Rietveld refinement of XRD patterns has been carried out with MAUD software [28].

The Infrared spectra (2 cm^{-1} resolution, average on 1024 scans) were collected in Attenuated Total Reflection (ATR) mode on loose powder with a Bruker Alpha-P spectrometer equipped with a germanium detector. All the spectra were recorded in a protected atmosphere (MBraun Lab Star Glove Box supplied with pure 5.5 grade Nitrogen, <0.01 ppm O_2, <0.01 ppm H_2O).

Thermo Gravimetric Analysis (TGA) experiments were performed with a Netzsch STA 449 F3 Jupiter instrument. Samples were measured in Al crucibles with pierced lids of the same material. The samples were heated between 30 °C and 600 °C, with a heating rate of 2 °C min^{-1} under argon gas (50 ml/min). The measurements were baseline corrected by the Proteus software package.

Temperature-Programmed Desorption (TPD) were measured in an in-house developed setup under vacuum (10^{-5} mbar) and between RT and 600 °C with a constant heating rate of 2 °C min^{-1}. Simultaneous Residual Gas Analysis (RGA) was measured with a MULTIVISON IP detector system coupled to a PROCESS Eye analysis package from MKS Instruments.

Hydrogen sorption treatments were obtained in the 0 – 100 bar pressure range using a volumetric instrument (PCI instrument by Advanced Materials Corporation, Pittsburgh PA). Ultra-pure 6.0 grade H_2 was used and the powders (about 500 mg) were transferred under nitrogen atmosphere in the measurement cell.

Results and discussion

Some inconsistencies can be found in the literature between the experimental [29] and theoretical [30] phase stability in $Mg(BH_4)_2$. The PBE functional was not able to predict the α-phase (space group $P6_122$) as the most stable. On the contrary, results of calculations obtained with the PBE-D* method confirm that a proper description of the dispersive forces (i.e. London forces, also known as instantaneous dipole-induced dipole forces) are crucial to predict the correct order of phase stability, as already observed in previous calculations [11]. To generate the $Mg_{(1-x)}Zn_x(BH_4)_2$ solid solutions, α-phase of $Mg(BH_4)_2$ has been considered, with a replacement of Mg^{2+} with Zn^{2+} ions, without

lowering the symmetry of the crystalline structure. An enthalpy of mixing close to zero has been calculated for all compositions and the results are shown in figure 1a. Because of possible different configurations of Mg-to-Zn substitutions, different values are reported for the same composition. The interaction between Mg^{2+} and BH_4^- in α-$Mg(BH_4)_2$ is basically covalent, as evidenced by the directionality of the chemical bond. On the other hand, the substitution of Mg^{2+} with Zn^{2+}, which display different values of electronegativity, does not involve relevant lattice distortions, suggesting the introduction of an ionic character in the bond. Calculated volumes of solid solutions are reported in figure 1b as function of the Zn molar fraction: it is evident that the addition of Zn into α-$Mg(BH_4)_2$ is predicted to cause a contraction of the volume cell, with an almost linear trend.

The results suggest an ideal trend for the solid solution. Considering an ideal entropy, a negative free energy of mixing can be estimated at room temperature for all compositions, suggesting the tendency of the system to form solid solutions. On the basis of DFT results, the enthalpy of decomposition of solid solutions has been estimated, considering MgH_2, Zn, B and H_2 as products, and a value of 30 $kJ \cdot mol^{-1}_{H2}$ has been calculated for x = 0.2.

In order to verify the results of calculations, mixtures of $Mg(BH_4)_2$ and $ZnCl_2$ with 1:0.7 ratio have been ball milled in different conditions. Pure compounds have been milled at room temperature for 12 hours (S1) and 45 minutes (S2), as well as in cryo-milling conditions for 1 hour (S3).

Experimental XRD patterns of as-milled powders are shown in figure 2 (points), together with those refined by Rietveld method (lines). The pattern obtained from a gently mixed mixture is reported as a reference (pattern a). In all ball milled samples the formation of Zn and $MgCl_2$ is observed, but the phase mixture obtained after the synthesis strongly depends on the milling conditions. For prolonged milling times (S1 sample, 12 hours of ball milling, pattern b), the presence of only Zn and $MgCl_2$ has been observed, suggesting the delivering of B-containing gaseous species, as confirmed by a slight increase of pressure inside the vial during ball milling. The occurrence of an extra broad peak around 2θ = 32° might suggest also the formation of amorphous B-containing phases during ball milling. Reducing the milling time at room temperature (S2 sample, 45 minutes of ball milling, pattern c), diffraction peaks of α-$Mg(BH_4)_2$ can be observed, together with those of Zn and $MgCl_2$. Even in this case, a proper fitting of experimental pattern can be obtained considering an extra broad peak around 2θ = 32°. From the Rietveld refinement of XRD pattern (R_W=13%), the lattice constants of tetragonal α phase turned out equal to a = 10.147 Å and c = 36.398 Å, slightly lower than those of the pure compound determined as a = 10.336 Å and c = 37.089 Å [29]. In this case, a volume contraction of 5.4 % is obtained, suggesting the formation of a solid solution. In addition, for the refinement of peak intensities, a Mg-to-Zn substitution in the structure was necessary. Taking the calculated volume contraction as a reference (figure 1b), a Zn-

content with x around 0.7 can be estimated. Performing the synthesis in cryo-conditions (S3 sample, 1 hour of ball milling, pattern d), a reduction of reaction yield is obtained. In fact, diffraction peaks of $ZnCl_2$ are still present in the XRD pattern, together with those of α-$Mg(BH_4)_2$, Zn and $MgCl_2$. In this case, lattice constants of tetragonal α phase obtained from Rietveld refinement (R_W=6%), are a = 10.216 Å and c = 36.673 Å, suggesting a value of x around 0.4 in the solid solution, close to the calculated optimal composition for H_2 delivering around room temperature (x = 0.2).

ATR spectra for as milled samples are reported in figure 3, together with that of pure α-$Mg(BH_4)_2$ taken as a reference (curve a). All samples show the typical absorption bands corresponding to the stretching and bending vibration of B-H in the regions between 2200 and 2400 cm^{-1} and 1100 and 1300 cm^{-1}, respectively. The peaks due to these vibration modes are basically at the same position for all the as-milled samples and are very similar to those observed for pure α-$Mg(BH_4)_2$ but they appear broader, likely due to microstructure refinement because of the ball milling process. Sample S1 (curve b) also shows ATR peaks, related to BH_4^- groups in the sample, possibly due to species present in the amorphous phase. For S2 and S3 samples (curves c and d), the formation of a shoulder at about 2180 cm^{-1} can be clearly observed, together with a splitting of the peak at about 790 cm^{-1}. These features indicate a larger heterogeneity of the BH_4^- groups in the structure of α-$Mg(BH_4)_2$ for these samples, possibly correlated to the incorporation of Zn^{2+} into the structure.

The results of TGA measurements on as-milled samples are reported in figure 4, where the signal obtained from pure α-$Mg(BH_4)_2$ is also reported as a reference (curve a). For sample S1 (curve b), a continuous mass loss is observed after heating, reaching a maximum value of about 4% at 450 °C. This result confirms the presence of hydrogenated species in the sample, which desorb a gas phase during heating. Samples S2 and S3 show a much higher mass loss, which begins well below 100 °C and continues up to the maximum heating temperature. The total mass loss turned out equal to about 12% and 10% for samples S2 (curve c) and S3 (curve d), respectively. These numbers are rather high, taking into account the presence of non-hydrogenated phases (Zn, $MgCl_2$ and $ZnCl_2$), suggesting the delivering of B-containing gas species upon heating.

In order to identify the composition of the gas phase desorbed by the samples during heating, TPD-RGA measurements were performed and the results are reported in figure 5. Only data for mass 2 (H_2) and 26 (B_2H_6) are reported, because of the negligible intensity observed for other masses. The result obtained for pure α-$Mg(BH_4)_2$ (figure 5a) confirms the delivering of a significant amount of H_2, starting at about 250 °C and with a desorption peak around 300 °C, whereas basically no B_2H_6 desorption is observed. On the contrary, ball milled samples show a hydrogen release for temperatures lower than 100 °C, suggesting a significant decrease of the decomposition temperature with respect to pure $Mg(BH_4)_2$. Sample S1 (figure 5b) shows a H_2 release distributed in a wide

temperature range, from 100 °C up to 450 °C, coupled with a small release of B_2H_6 at low temperatures. B_2H_6 delivering is much stronger for S2 sample (figure 5c) and it seems to be coupled with H_2 release up to about 250 °C, whereas at higher temperatures only H_2 is observed in the gas phase. Finally, for S3 sample (figure 5d) a clear three-step desorption process is observed, with a significant B_2H_6 delivering around 100 °C. Results obtained from TPD-RGA measurements are in good agreement with those obtained by TGA. The high mass loss observed around 100 °C during thermal decomposition is clearly related to the delivering of B_2H_6. This observation supports the presence of Zn cations into the α-$Mg(BH_4)_2$ structure, which forms weak bonds with B, promoting the formation of B_2H_6.

In order to identify the reaction steps occurring in sample S3, portion of the sample were heated under 0.1 bar of H_2 up to selected temperatures, corresponding to the end of H_2 desorption peaks observed in figure 5d. An enlarged view of the results of XRD analysis of samples desorbed at 125 °C, 200 °C and 350 °C are reported in figure 6, where the pattern of as-milled sample is also reported for comparison (pattern a). After heating up to 125 °C (pattern b), the mixture of crystalline phases was rather similar to that present in the as-milled sample, i.e. Zn, $MgCl_2$, α-$(Mg,Zn)(BH_4)_2$ solid solution and residual $ZnCl_2$. After heating up to 200 °C (pattern c), the α-$(Mg,Zn)(BH_4)_2$ solid solution nearly disappeared and the amount of Zn and $MgCl_2$ slightly increased. Finally, after heating up to 350 °C (pattern d), a small amount of $MgZn_2$ Laves phase was observed. Rehydrogenation for 16 hours under 100 bar H_2 has been attempted on sample S3 after dehydrogenation and the corresponding XRD patterns are shown in figure 6 for samples treated at 125 °C (pattern e) and 200 °C (pattern f). It is clear that the dehydrogenation reaction is not reversible for this sample, likely due to the B_2H_6 desorption at low temperatures.

Experimental results can be discussed on the basis of the possible reaction paths, as estimated from available thermodynamic databases. The results of a thermodynamic modeling for the mixture $Mg(BH_4)_2$ + $ZnCl_2$ show that, in the 100-350 °C temperature range, thermodynamically stable phases are a series of magnesium borides, metallic Zn, $MgCl_2$ and the gas phase, mainly composed of H_2. According to the calculations, diborane should not be released in the gas phase. If the release of B-containing species in the gaseous phase is to be considered, all condensed phases containing boron must be suspended from the calculations. This can be possible either if their formation is hindered for kinetic reasons or because boron is removed from the material during thermal desorption. At high temperatures (around 350 °C), Mg atoms remaining from the decomposition of magnesium borohydride are allowed to form the $MgZn_2$ compound, as observed experimentally. Even if an anion substitution cannot be excluded, this result suggests a very close presence of Mg

and Zn atoms in the ball milled materials, supporting the formation of $Mg_{(1-x)}Zn_x(BH_4)_2$ solid solutions.

Conclusions

On the basis of DFT calculations, an ideal mixing behaviour was predicted for $Mg_{(1-x)}Zn_x(BH_4)_2$ solid solutions with the same structure of α-$Mg(BH_4)_2$. The enthalpy of decomposition of solid solutions has been estimated, considering MgH_2, Zn, α-B and H_2 as products, and a value of 30 $kJ \cdot mol^{-1}_{H2}$ has been calculated for x=0.2. Samples have been synthesized ball milling $Mg(BH_4)_2$ and $ZnCl_2$ in a molar ratio 1:0.7 with different conditions and characterized using with a combination of experimental techniques (XRD, ATR, TGA, TPD-RGA).

Experimental results showed that a $Mg_{(1-x)}Zn_x(BH_4)_2$ solid solution with x = 0.4 and 0.7 is formed for the investigated milling conditions. Under heating, a significant amount of B_2H_6 is released already at low temperatures, preventing the reversibility of hydrogen sorption. Thermodynamic calculations predicted magnesium borides, Zn and $MgCl_2$ as stable dehydrogenation products, with no release of diborane in the gas phase. The presence of diborane could only be obtained rejecting all the compounds containing boron from the database, as if their formation would be hindered.

Acknowledgments

The research leading to these results has received funding from the Fuel Cells and Hydrogen Joint Undertaking under SSH2S grant agreement n° 256653.

References

[1] L.H. Rude, T.K. Nielsen, D.B. Ravnsbaek, U. Bosenberg, M.B. Ley, B. Richter, L.M. Arnbjerg, M. Dornheim, Y. Filinchuk, F. Besenbacher, T.R. Jensen, Tailoring properties of borohydrides for hydrogen storage: A review, Physica Status Solidi a-Applications and Materials Science, 208 (2011) 1754-1773.

[2] S.I. Orimo, Y. Nakamori, J.R. Eliseo, A. Zuttel, C.M. Jensen, Complex hydrides for hydrogen storage, Chem. Rev., 107 (2007) 4111-4132.

[3] H.W. Li, S. Orimo, Y. Nakamori, K. Miwa, N. Ohba, S. Towata, A. Zuttel, Materials designing of metal borohydrides: Viewpoints from thermodynamical stabilities, J. All. Compd., 446 (2007) 315-318.

[4] H.W. Brinks, A. Fossdal, B.C. Hauback, Adjustment of the stability of complex hydrides by anion substitution, J. Phys. Chem. C, 112 (2008) 5658-5661.

[5] J.E. Fonnelop, M. Corno, H. Grove, E. Pinatel, M.H. Sorby, P. Ugliengo, M. Baricco, B.C. Hauback, Experimental and computational investigations on the AlH_3/AlF_3 system, J. All. Compd., 509 (2011) 10-14.

[6] S. Hino, J.E. Fonnelop, M. Corno, O. Zavorotynska, A. Damin, B. Richter, M. Baricco, T.R. Jensen, M.H. Sorby, B.C. Hauback, Halide Substitution in Magnesium Borohydride, J. Phys. Chem. C, 116 (2012) 12482-12488.

[7] D.B. Ravnsbaek, L.H. Rude, T.R. Jensen, Chloride substitution in sodium borohydride, J. Solid State Chem., 184 (2011) 1858-1866.
[8] L.H. Rude, Y. Filinchuk, M. Sorby, B. Hauback, T. Jensen, Effect of anion substitution in metal borohydrides, Abstracts of Papers of the American Chemical Society, 240 (2010).
[9] L.H. Rude, Y. Filinchuk, M.H. Sorby, B.C. Hauback, F. Besenbacher, T.R. Jensen, Anion Substitution in $Ca(BH_4)_2$-CaI_2: Synthesis, Structure and Stability of Three New Compounds, J. Phys. Chem. C, 115 (2011) 7768-7777.
[10] L.H. Rude, E. Groppo, L.M. Arnbjerg, D.B. Ravnsbaek, R.A. Malmkjaer, Y. Filinchuk, M. Baricco, F. Besenbacher, T.R. Jensen, Iodide substitution in lithium borohydride, $LiBH_4$-LiI, J. All. Compd., 509 (2011) 8299-8305.
[11] L.H. Rude, O. Zavorotynska, L.M. Arnbjerg, D.B. Ravnsbaek, R.A. Malmkjaer, H. Grove, B.C. Hauback, M. Baricco, Y. Filinchuk, F. Besenbacher, T.R. Jensen, Bromide substitution in lithium borohydride, $LiBH_4$-LiBr, Int. J. Hydrog. Energy, 36 (2011) 15664-15672.
[12] I. Llamas-Jansa, N. Aliouane, S. Deledda, J. E. Fonneløp, C. Frommen, T. Humphries, K. Lieutenant, S. Sartori, M.H. Sørby, B.C. Hauback, Chloride substitution induced by mechano-chemical reactions between $NaBH_4$ and transition metal chlorides, J. Alloy. Compd., 530 (2012) 186-192.
[13] J.E. Olsen, M.H. Sørby, B.C. Hauback, Chloride-substitution in sodium borohydride, J. Alloy. Compd., 509 (2011) L228-L231.
[14] C. Frommen, M.H. Sorby, P. Ravindran, P. Vajeeston, H. Fjellvag, B.C. Hauback, Synthesis, Crystal Structure, and Thermal Properties of the First Mixed-Metal and Anion-Substituted Rare Earth Borohydride $LiCe(BH_4)_3Cl$, J. Phys. Chem. C, 115 (2011) 23591-23602.
[15] R. Cerny, N. Penin, V. D'Anna, H. Hagemann, E. Durand, J. Ruzicka, $Mg_xMn(1-_x)(BH_4)_2$ (x=0-0.8), a cation solid solution in a bimetallic borohydride, Acta Mater. 59 (2011) 5171-5180.
[16] F. Fang, Y.T. Li, Y. Song, J. Zha, B. Zhao, D.L. Sun, $LiMn(BH_4)_3$/2LiCl Composite Synthesized by Reactive Ball-Milling and Its Dehydrogenation Properties, Acta Phys.-Chim. Sin., 27 (2011) 1537-1542.
[17] F. Fang, Y.T. Li, Y. Song, D.L. Sun, Q.G. Zhang, L.Z. Ouyang, M. Zhu, Superior Destabilization Effects of MnF_2 over $MnCl_2$ in the Decomposition of $LiBH_4$, J. Phys. Chem. C, 115 (2011) 13528-13533.
[18] J. S. Hummelshøj et al., Density functional theory based screening of ternary alkali-transition metal borohydrides: A computational material design project, J. Chem. Phys. 131 (2009) 014101.
[19] D. Ravnsbaek, Y. Filinchuk, Y. Cerenius, H. J. Jakobsen, F. Besenbacher, J. Skibsted, T. R. Jensen, A series of mixed-metal borohydrides, Angew. Chem. Int. Ed. 48 (2009) 6659-6663.
[20] E. Jeon, Y.W. Cho, Mechanochemical synthesis and thermal decomposition of zinc borohydride, J. Alloys Compd. 422 (2006) 273 – 275.
[21] J. P. Perdew, K. Burke, M. Ernzerhof, Generalized Gradient Approximation Made Simple, Phys. Rev. Lett. 77 (1996) 3865.
[22] S. Grimme, Semiempirical GGA-type density functional constructed with a long-range dispersion correction, J. Comput. Chem. 27 (2006) 1787–1799.
[23] B. Civalleri, C. M. Zicovich-Wilson, L. Valenzano, P. Ugliengo, Cryst. Eng. Comm. 10 (2008) 405-410.
[24] R. Dovesi, R. Orlando, B. Civalleri, C. Roetti, V. R. Saunders, and C. M. Zicovich-Wilson, CRYSTAL: a computational tool for the ab initio study of the electronic properties of crystals, Z. Kristallogr. 220 (2005) 571-573.

[25] R. Dovesi, V. R. Sauders, C. Roetti, R. Orlando, C. M. Zicovich-Wilson, F. Pascale, B. Civalleri, K. Doll, N. M. Harrison, I. J. Bush, P. D'Arco, M. Llunell, CRYSTAL09, University of Torino, Torino (2009).
[26] S. H. Lee, V. R. Manga and Z.-K. Liu, Effect of Mg, Ca, and Zn on stability of LiBH4 through computational thermodynamics, Int. J. Hydrog. Energy, 35 13 (2010) 6812-6821.
[27] SGTE substance database, Thermodynamic properties of inorganic materials. Landolt-Börnstein Group IV (Physical Chemistry), vol 19, Springer, Berlin (2003)
[28] L. Lutterotti, S. Matthies, and H.-R. Wenk, MAUD: a friendly Java program for material analysis using diffraction, IUCr: Newsletter of the CPD, 21 (1999) 14-15.
[29] Y. Filinchuk, R.Cerny, H.Hagemann, Insight into $Mg(BH_4)_2$ with synchrotron X-ray diffraction: structure revision, crystal chemistry and anomalous thermal expansion, Chem. Mat. 21(2009) 925-933.
[30] J. Voss, J. S. Hummelshøj, Z. Łodziana, T. Vegge, Structural stability and decomposition of $Mg(BH_4)_2$ isomorphs—an ab initio free energy study, Condens. Matter 21 (2009) 012203.

Figure captions

Figure 1. Calculated enthalpy of mixing of $Mg_{(1-x)}Zn_x(BH_4)_2$ solid solutions (a) and volume change of unit cell (b) as a function of Zn molar fraction. The error bars represent the estimated error of the computational method ($\approx \pm 1.5$ kJ/mol, see text). The dashed line indicates the ideal behaviour.

Figure 2. X-ray diffraction patterns (Cu K_α 1.540598 Å) of a gently mixed $Mg(BH_4)_2$ + 0.7 $ZnCl_2$ mixture (a) and of samples S1 (b), S2 (c) and S3 (d). Points: selected experimental data; lines: Rietveld refined pattern. Intensity is reported in logarithmic scale. Peak positions of $Mg(BH_4)_2$ (hexagonal-$P6_122$), $ZnCl_2$ (orthorhombic-$Pna2_1$), Zn (hexagonal-$P6_3/mmc$) and $MgCl_2$ (trigonal-$R\bar{3}m$) are shown as a reference.

Figure 3. ATR spectra of pure α-$Mg(BH_4)_2$ (a) and of samples S1 (b), S2(c) and S3 (d).

Figure 4. TGA profiles of pure α-$Mg(BH_4)_2$ (a) and of samples S1 (b), S2(c) and S3 (d).

Figure 5. TPD-RGA profiles of pure α-$Mg(BH_4)2$ (a) and of samples S1 (b), S2 (c) and S3 (d). Continuous line is used for mass 2 (H_2) and dashed line for mass 26 (B_2H_6). The temperature ramps used for the desorption is indicated by dotted lines.

Figure 6. X-ray diffraction patterns (Cu K_α 1.540598 Å) of sample S3 as-milled (a), dehydrogenated at 125°C (b), 200°C (c), 350°C (d), dehydrogenated and soaked into 100 bar of H_2 at 125°C (e) and 200°C (f). All patterns have been normalized with respect to the intensity of the peak at 15°. Peak positions are shown as a reference.

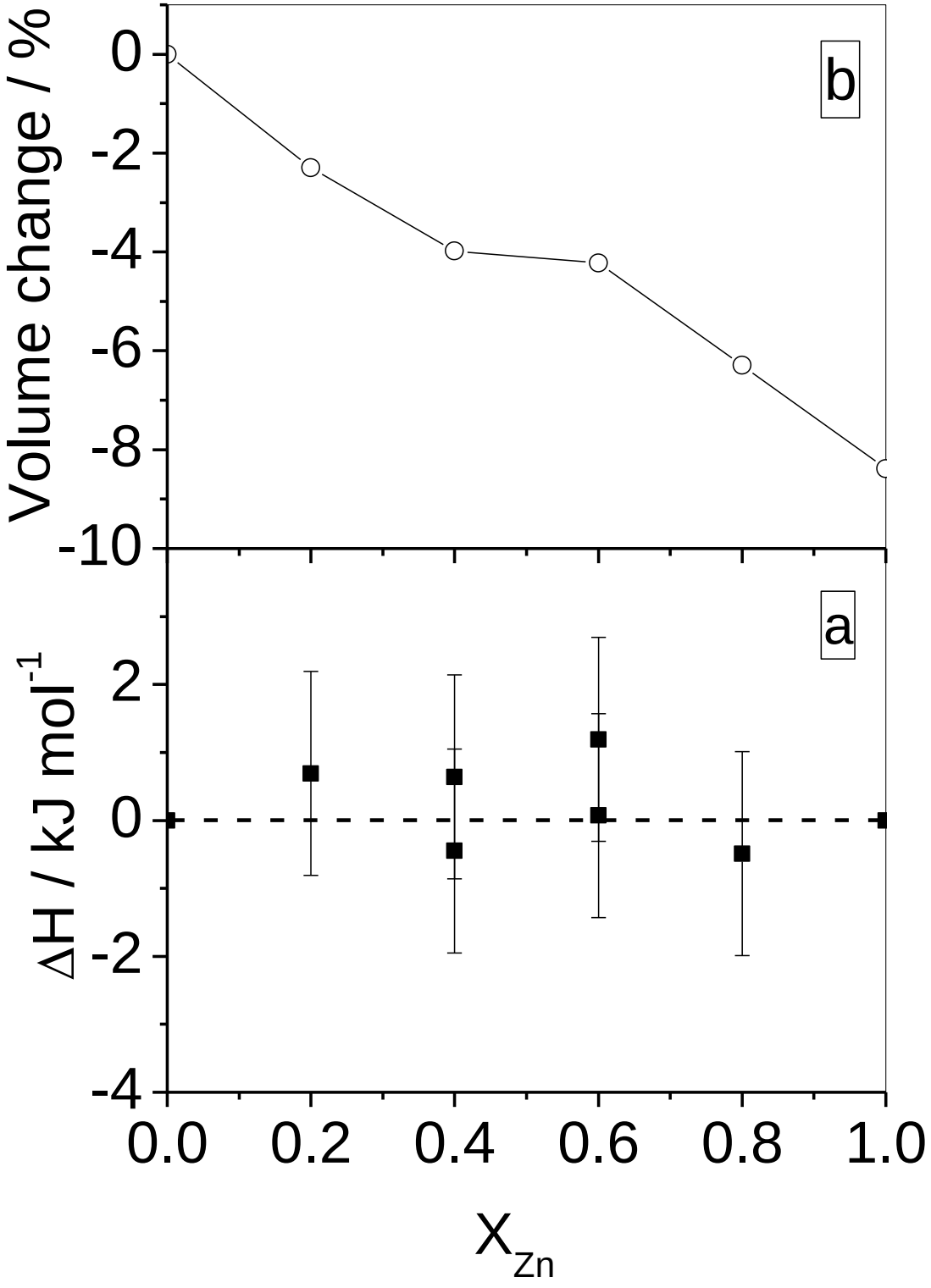

Figure 1

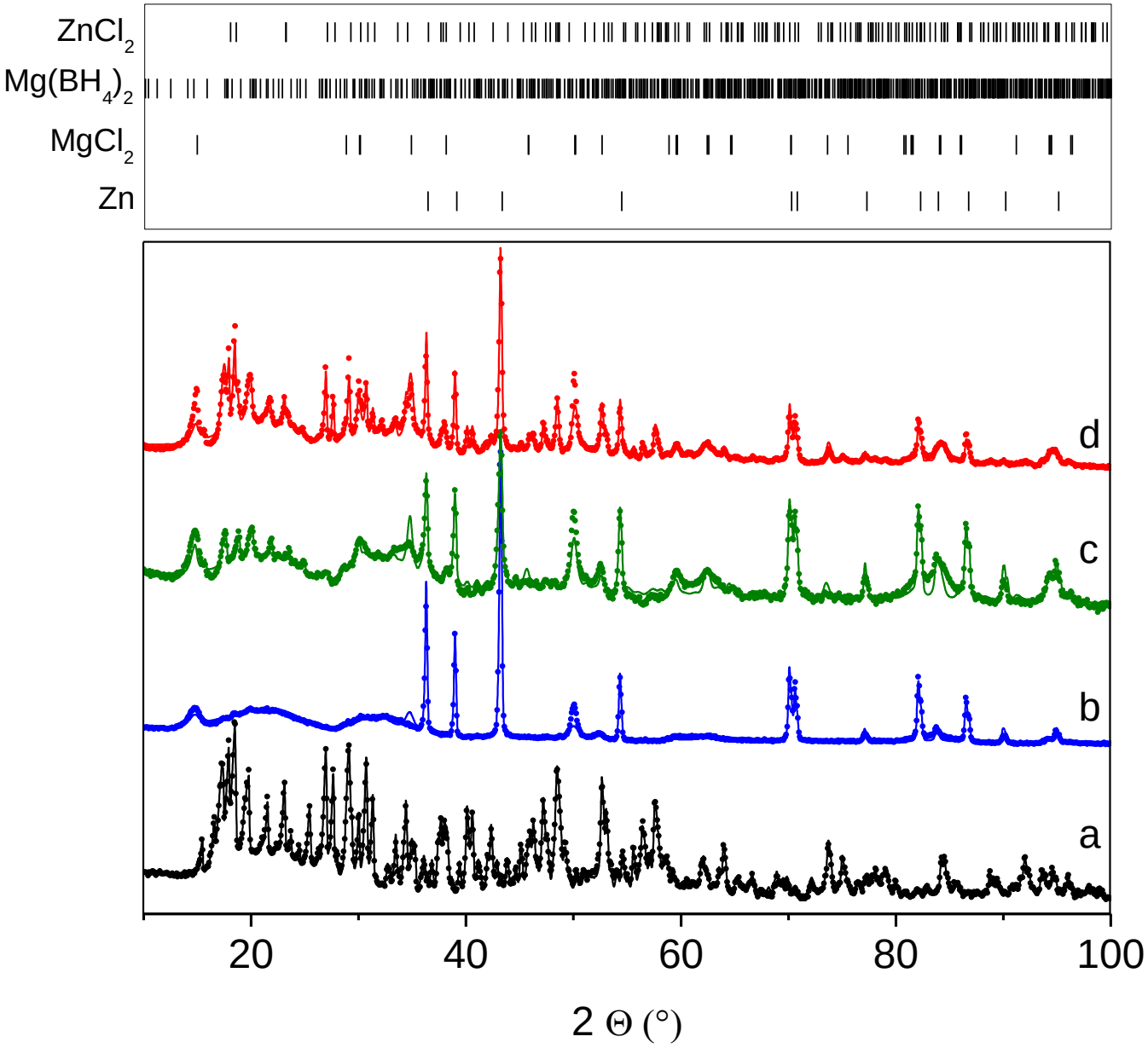

Figure 2

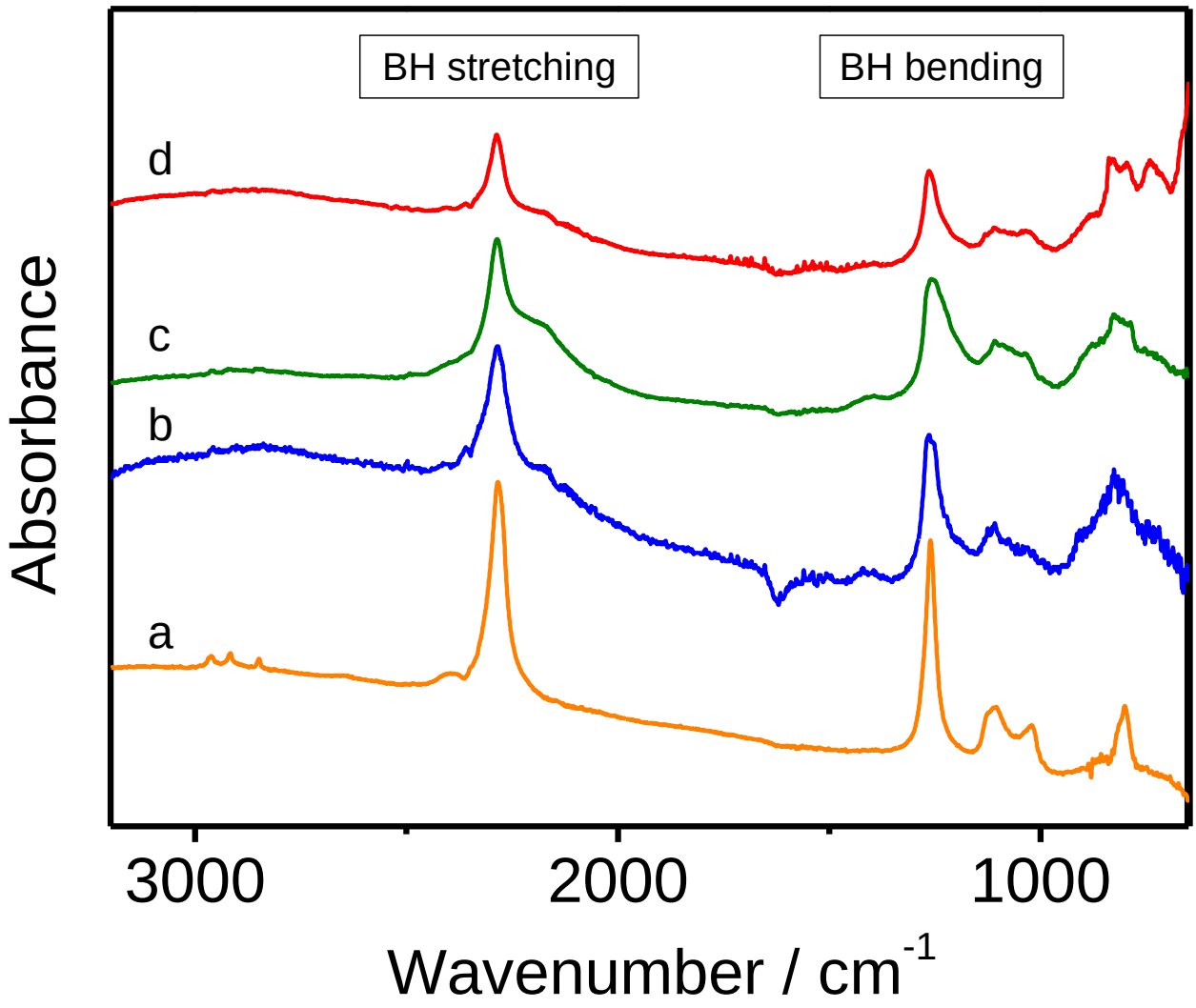
BH stretching
BH bending
d
c
b
a
Absorbance
3000
2000
1000
Wavenumber / cm-1

Figure 3

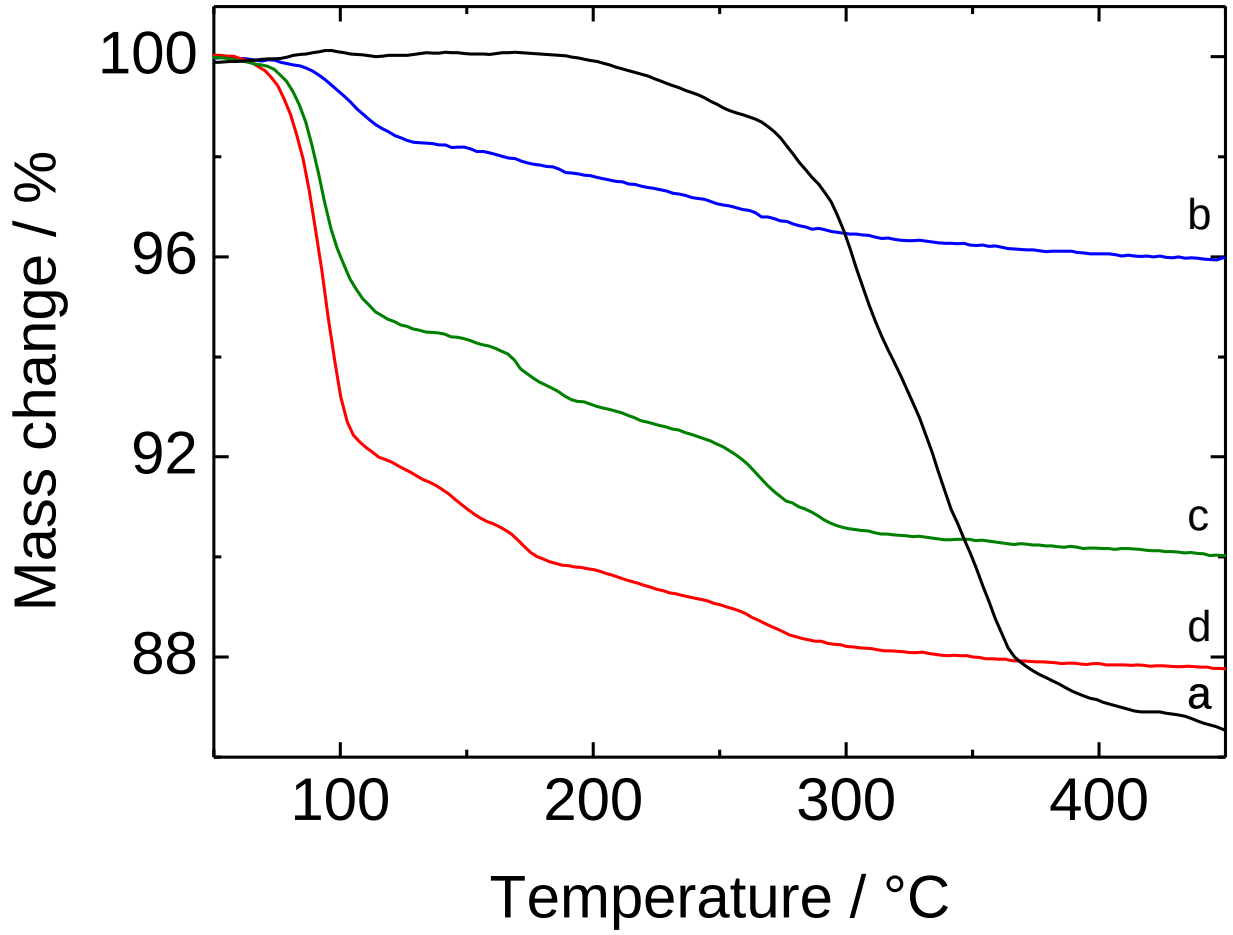

Figure 4

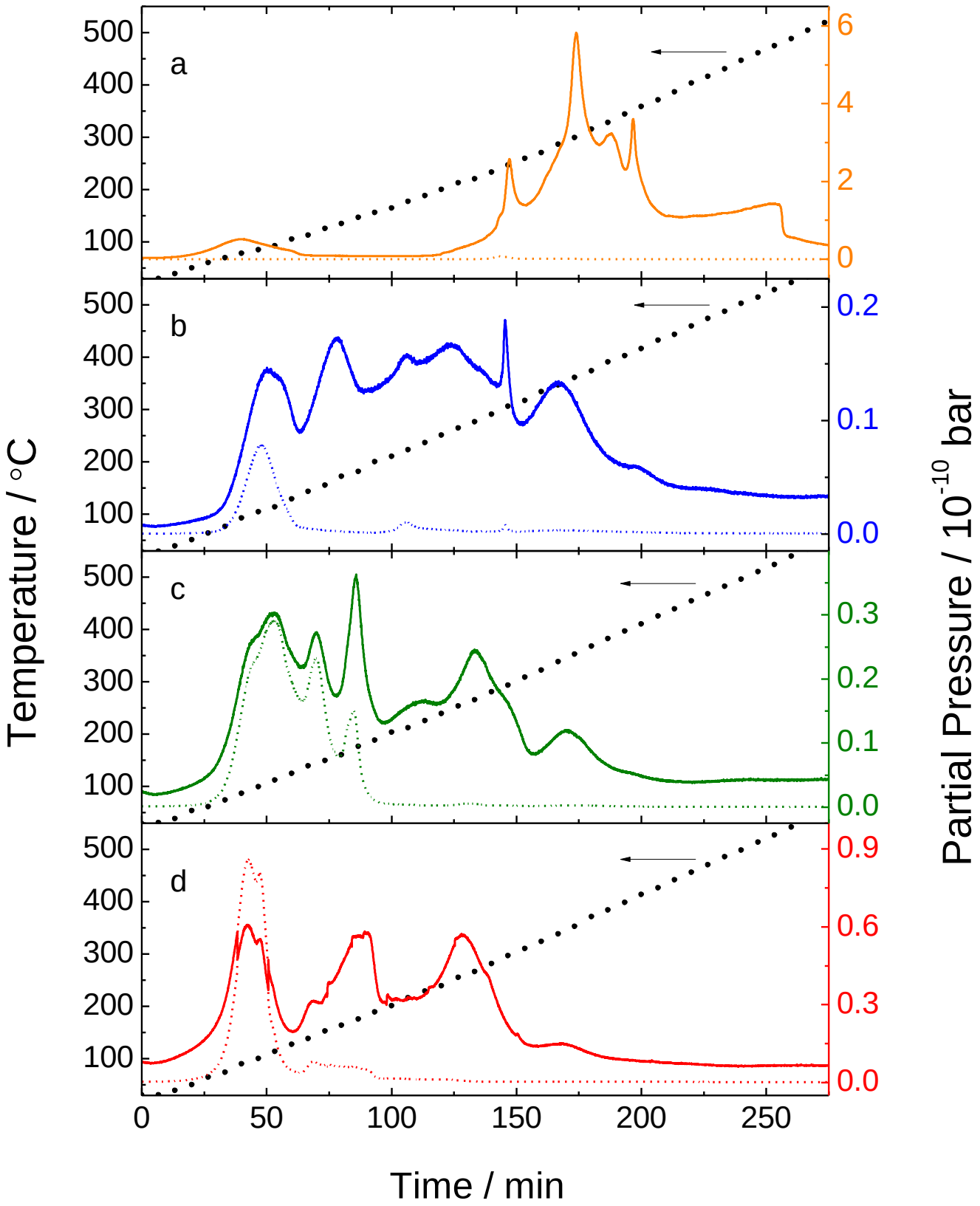
a
b
c
d
Temperature / °C
Partial Pressure / 10-10 bar
Time / min
500
400
300
200
100
0
50
100
150
200
250
6
4
2
0
0.2
0.1
0.0
0.3
0.2
0.1
0.0
0.9
0.6
0.3
0.0

Figure 5

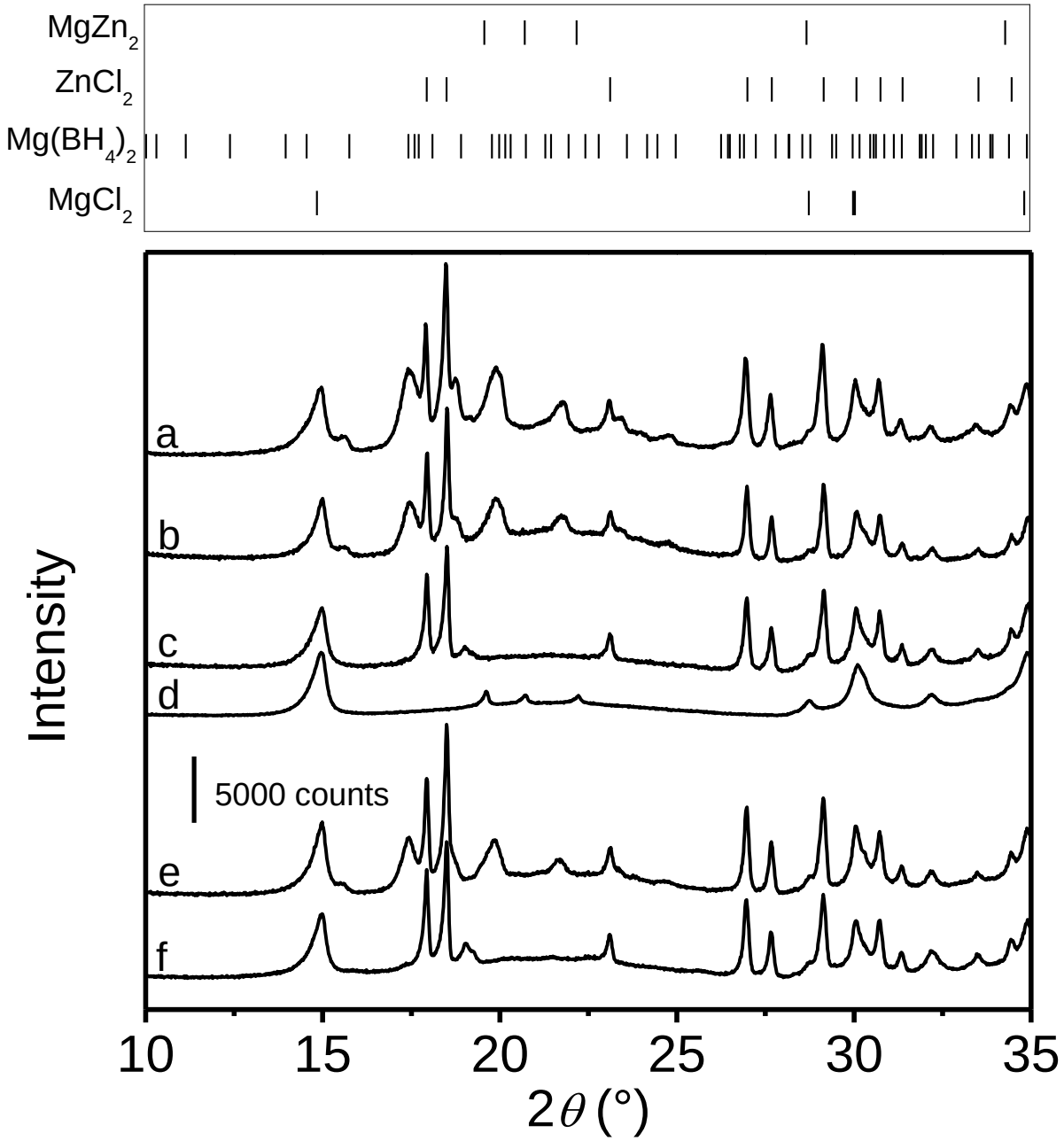
MgZn2
ZnCl2
Mg(BH4)2
MgCl2
a
b
c
d
e
f
5000 counts
Intensity
10
15
20
25
30
35
2θ (°)

Figure 6